Use of CFD For Design Validation of A Transonic Civil Transport

Honam Ok*, Insun Kim, Seong-Wook Choi* and Bongzoo Sung****
Aerodynamics Department
Korea Aerospace Research Institute, Korea 305-333

Abstract

The applications of CFD in the design process of a transonic civil transport at Korea Aerospace Research Institute (KARI) are outlined. Three Navier-Stokes solvers, developed at KARI with different grid approaches, are used to predict the aerodynamic coefficients and solve the flowfield of various configurations. Multi-block, Chimera, and unstructured grids are the approaches implemented. The accuracy of the codes is verified for the transonic flow about RAE wing/fuselage configuration. The multi-block code is used to provide the detailed data on the flowfield around a wall interference model with different test section sizes which will be used in establishing the wall interference correction method. The subsonic and transonic flowfields about K100-04A, one of the configurations of a 100-seater transport developed by KARI and Korea Commercial Aircraft Development Consortium (KCDC), are computed to predict the aerodynamic coefficients. The results for the subsonic flow are compared with those of wind tunnel test, and the agreement is found to be excellent. The interference effect of nacelle installation on the wing of K100-04A is also investigated using the unstructured grid method, and about 10% reduction in wing lift is observed. The accuracy of the three developed codes is verified, and they are used as an efficient tool in the design process of a transonic transport.

Key Word : CFD, design, validation, transonic, civil, transport

Introduction

Recent progresses in the field of computational fluid dynamics (CFD) has made it an essential part of aircraft design tools. The development of more efficient and accurate solution algorithms together with advances in computing power, memory capacity and networking speed has made it more cost-effective to use CFD than to resort to the wind tunnel tests in some phases of aircraft design. Computations of three-dimensional flows over simple realistic aerodynamic configurations were made by many groups worldwide using structured grids, but structured grid generation about complex configurations still remains as a serious challenge.[1]

In multi-block approach, this problem is solved by dividing the whole flow region into multiple blocks.[2] Blocked grids as presented here have complete continuity of grid lines across block boundaries. Another approach is to generate independent sets of structured grids about each component while allowing overlap and is called overset or Chimera grid.[3] These two approaches have been widely used for the computations of the viscous flows over complex configurations, and the more automated generation of multiblock and Chimera grids have been possible. A totally different approach that has become popular recently is to fill the flowfield with unstructured grids composed of simplices like triangles in two dimensions and tetrahedra in three dimensions. Recent progresses have shown that the accuracy and efficiency of unstructured methods are comparable to those by the structured

* Senior Researcher
** Principal Researcher

grid methods for inviscid flow calculations.[1]

In the preliminary design stage of an aircraft, established analytic or empirical methods[4,5] are commonly used to compute the aerodynamic coefficients with acceptable accuracy if certain constraints are satisfied. However, it is not rare for subsonic and transonic flows that some of the constraints are not met and the predicted aerodynamic coefficients can possibly have considerable errors. For an accurate prediction of aircraft performance, it is essential to have precise estimation of the aerodynamic characteristics of the aircraft and more accurate methods are required for this purpose.

For the development of a 100-seater transport in Korea, a joint design team was organized by Korea Aerospace Research Institute (KARI) and Korea Commercial Aircraft Development Consortium (KCDC). Most of the design works have been done by this group of engineers, and K100-04A is one of the configurations of the aircraft evolving with design modifications. It is one of the most important roles of KARI in this development project to validate whether the design requirements are satisfied and what modifications should be made otherwise. For the aerodynamic validations, wind tunnel test and/or CFD analysis can be employed. As for the wind tunnel testing, a screen test was performed at a low speed wind tunnel with the test section of 1m×0.7m.[13] To achieve larger Reynolds number with the same test section size, a good method of wall interference correction is indispensable. A detailed information on the flowfields with different test section wall sizes will be helpful in establishing a wall correction method, and this is also done by the use of CFD in addition to the design validation mentioned above.

In this paper, outlined is the effort using CFD for accurate prediction of the aerodynamic coefficients of an aircraft in the preliminary design stage together with the prediction of the flowfield under the influence of wall interference. Three Navier-Stokes codes, employing multi-block, overset, and unstructured grid methods, were developed at KARI and have been used for various applications.[6,7,14] The accuracy of the codes for transonic flows is demonstrated by comparison with the experimental data of the transonic flowfield about RAE wing/fuselage configuration.[10] Then, the multi-block code is applied to predict the wall interference on the flowfield around the model with different test section sizes. The Chimera overset grid solver is applied to provide the aerodynamic performance data of wing/fuselage/tail configuration of K100-04A for both subsonic and transonic flow conditions. Finally, the installed nacelle effect on the aerodynamic characteristics of the wing is estimated using the unstructured grid method.

Numerical Methods

The three Navier-Stokes codes used in this paper are described briefly below. Two structured grid codes, PENS3D and XM3D, were developed by KARI, and the development of the unstructured grid code, UNS3D, was supported by KARI.

PENS3D solves the three-dimensional compressible Navier-Stokes equations for a body-fitted coordinate system using multi-block grid approach.[6] The equations are discretized using a finite-volume formulation, and the convective terms are upwind-biased using the flux difference splitting of Roe. The resulting matrix equation is solved implicitly using a diagonalized three-factor approximate factorization while convergence is accelerated using multigrid technique. The viscous flux terms are discretized using central differences and the Baldwin-Lomax turbulence model is incorporated.

XM3D uses central differencing for the convective terms based on a finite-difference formulation.[7] It uses the Chimera grid approach, and a diagonalized three-factor approximate factorization is used to advance to steady state. XM3D also incorporates the viscous terms with the Baldwin-Lomax turbulence model to solve the Navier-Stokes equations.

UNS3D code is based on a cell-centered finite-volume formulation using unstructured grids composed of tetrahedra.[8] Roes flux difference splitting is used to discretize the convective terms, and the solution is advanced to steady state using multi-stage Runge-Kutta scheme. The convergence is further accelerated using residual smoothing. To obtain higher-order accuracy, the solution gradient

in a cell should be computed, and this is done by using geometric invariants as proposed by Frink.[9] This code also incorporates the central-differenced viscous terms with k-e turbulence model which is strongly coupled with the flow equations.

Results and Discussions

The accuracy of the three codes was first verified by comparing the results with the experimental data on RAE wing/fuselage configuration in a transonic flowfield. Then, the multi-block code, PENS3D, was used to provide the detailed data on the flowfield of wing/flap/fuselage/tail configuration to be used in establishing the wall interference correction method at KARI. The subsonic and transonic flowfields about K100-04A configuration were computed to predict the aerodynamic coefficients and the results were compared with those of wind tunnel tests. The dimensions of K100-04A are: body length 103.92 ft, wing span 96.4 ft, wing area 1,092 ft^2, aspect ratio 8.51, wing taper ratio 0.2345, leading edge sweep angle 26.75°, and the dihedral angle 5.717°. Lastly, the interference effect of nacelle mounting on the wing of K100-04A was investigated using the unstructured grid method.

RAE Wing/Fuselage Configuration

The transonic inviscid flowfield about RAE wing/fuselage configuration was calculated for Mach number 0.9 and angle of attack 1. In Figure 1, the computed pressure coefficients along the chord at selected spanwise locations are compared with those by experiment,[10] and the overall agreement with experiment is good for all three solvers. The pressure distribution on the lower wing surface is almost identical, but the predicted shock location and strength on the upper surface show small discrepancy between the solvers and experiment. The discrepancy between the solvers can be attributed to the differences in the spatial differencing schemes and the meshes. The unstructured grid solver, UNS3D, has clearest shock resolution due to the largest number of grid points near the region, but the Chimera grid solver, XM3D, shows the best overall agreement even with slightly smeared shock which is due to the use of central differencing. The pressure distribution on the body showed similar agreement with experimental results even though it is not shown here.

Wall Interference Model

In the wind tunnel test, the presence of test section walls inevitably influence the flowfield around the model, and the effect of the wall interference should be corrected somehow to correlate the wind tunnel test data to real flight condition without walls. Most wind tunnel sites provide test data which are corrected for wall interference effects, and some experiments[11] were done at NLR (National Aerospace Laboratory, the Netherlands) to evaluate their wall interference correction method. An effort is going on at KARI to establish its own wall interference correction method, and the NLR wall interference model was selected as a reference to evaluate the wall interference. The detailed information on the flowfield would help make corrections on wall interference effects, and turbulent flow calculations were done for this purpose.

The NLR wall interference model consists of horizontal tail and flap of NACA 0012 airfoil, main wing of NACA 4412 airfoil, and fuselage with

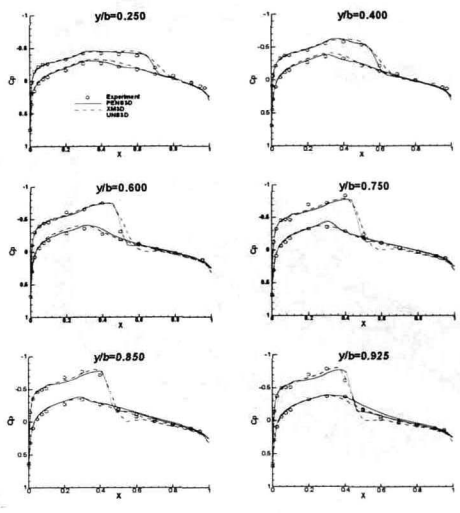

Fig. 1. Pressure Coefficient Distribution on the Wing of RAE Wing/Fuselage Configuration for M=0.9, α=1°

the nose of an epllipsoid and the body of a circular cylinder. The wall interference model of KARI retains the same features while wing position and flap configuration are not clearly stated in Reference 11. The test results with two test sections of NLR (small - 0.8m×0.6m, large - 3.0m×2.25m) are used here for comparison with computation. Twelve blocks of mesh were generated using a commercial grid generation package, Gridgen,[12] and only outer two blocks need to be regenerated according to the changes in the angle of attack. In Figure 2, the typical mesh is shown and the number of grid points is about 1 million for symmetric half of the domain for both test sections. The flow was computed for Mach number of 0.18, Reynolds number of 4×10^6, and the flap deflection angle of 20° as in the NLR test, and the angle of attack was set to 0° and 4°.

In Figure 3, the pressure coefficient distributions on main wing and flap is shown for 4° angle of attack, and the influence of test section size can be clearly seen. The influence of wall interference is more pronounced around the leading edge of the main wing, and it is almost negligible on the flap. On the fuselage, the influence can be only felt in the wing-fuselage junction, and this is believed to be due to the influence of wing pressure variation, not the direct effect of the presence of wind tunnel walls. Similar results as in Figure 3 were obtained for 0° angle of attack.

In Figure 4, computed lift and drag coefficients for both test section sizes are compared with those of NLR experiment. The results agree with each other qualitatively, and the lift coefficient is over-predicted with small test section while drag coefficient is under-predicted in both computation and experiment. The difference in aerodynamic coefficients for the two test section sizes increases as angle of attack is raised, and this is considered to be the result of larger increase in blockage ratio in smaller test section. The computed aerodynamic coefficients do not agree with those of NLR test exactly, but the effect of wall interference is well predicted.

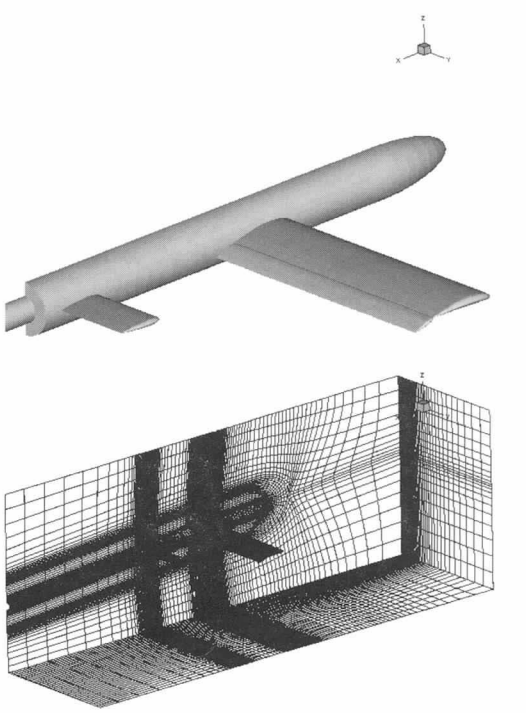

Fig. 2. Geometry and Mesh of KARI Wall Interference Model In Wind Tunnel Test Section

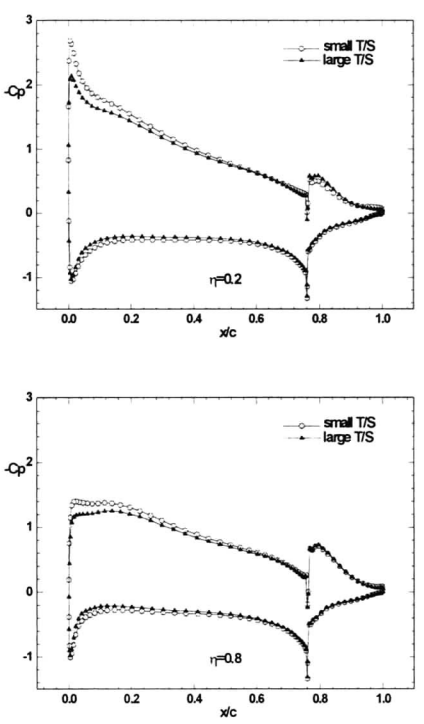

Fig. 3. Comparison of Pressure Coefficient Distributions on the Main Wing and Flap of NLR Wall Interference Model with Change of Test Section Size

Wing/Fuselage/Tail Configuration of K100-04A

As explained before, K100-04A is one of the 100-seater transonic transport configurations designed by KARI and Korean aerospace companies. Design modifications were made depending upon the result of the aerodynamic performance analysis using some empirical methods or CFD. In these preliminary design stages, CFD analysis played an important role in determining the aerodynamic performance of the aircraft. To verify the low-speed characteristics of the K100-04A configuration predicted by CFD, wind tunnel test was performed at KARI with 1/45 scale model,[13] and the results were compared.

The Chimera grid shown in Figure 5 was generated using Gridgen as for the KARI wall interference model and the surface mesh was projected onto the geometry of the configuration transferred from the CAD package in IGES format. C-O type meshes were generated for each of the four components of the configuration, which considerably reduced the labor of mesh generation, and the total number of nodes was about 1 million for the symmetric half of the flow domain.

First, the subsonic flow was computed to compare with wind tunnel test for Mach number of 0.3 and Reynolds number of 1.0×10^6, and the results are shown in Figure 6 together with those of the transonic flow prediction. Even though the computed drag coefficients are slightly lower than the experimental results and the stall is not predicted in the computed range of angle of attack, the overall agreement between the computation and experiment is excellent.

For transonic flows, no wind tunnel test was performed and the results by CFD analysis were

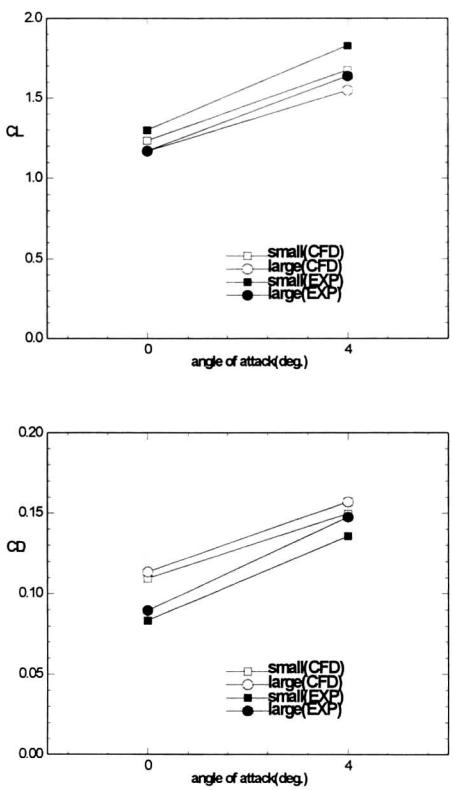

Fig. 4. Comparison of Predicted Aerodynamic Coefficients with NLR Wind Tunnel Test for Different Test Sections

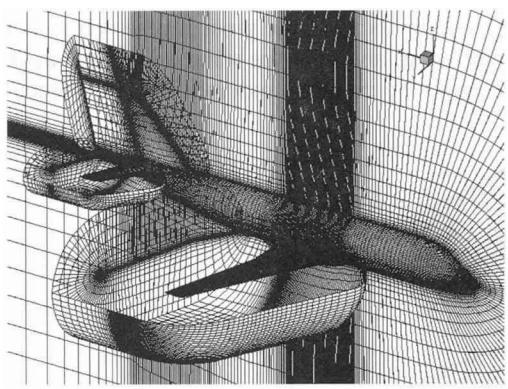

Fig. 5. Chimera Overset Grids Around Wing/Fuselage/Tail Configuration of K100-04A

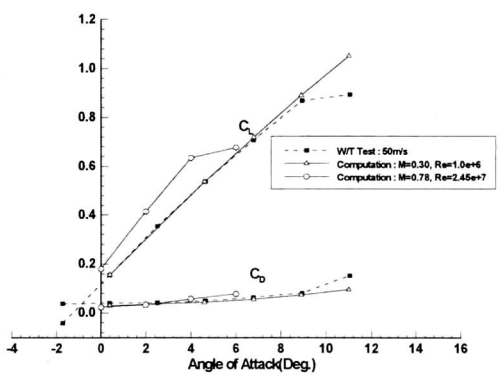

Fig. 6. Comparison of the Aerodynamic Coefficients for K100-04A Wing/Fuselage/Tail Configuration

accepted as a highly dependable source of information in determining the aerodynamic performance of the configuration judging from the previous results and other applications.[14] For transonic flows of Mach number 0.78 and Reynolds number of 2.45×10^7 which represents the cruise condition, the slope of lift coefficient curve suddenly decreases over the angle of attack of 4°. This is due to the shock-induced boundary layer separation as shown in Figure 7. The contour plots of pressure coefficient and the streamline patterns on the upper surface of wing are shown for computed angles of attack in this figure. Separation first occurs around the mid-span for lower angle of attack and the separated region extends to the root of wing for higher angle of attack. Wing tip still produces lift due to the nose-down twist at the tip section.

Wing Nacelle Interference of K100-04A

The installation of the engine should be optimized to get the best performance of the aircraft, and it is crucial to the wing designer to understand the interference effects. To optimize the integration of the engine, wind tunnel tests have been widely employed because the accuracy of the numerical codes is not good enough when viscous effects are dominant. Nevertheless, Euler codes can predict quite well the mean characteristics of the flow around an installed nacelle configuration.[15] For the preliminary design of K100-04A configuration, this interference effect is estimated using an unstructured Euler solver. The mesh generation around wing and nacelle requires too much effort with the structured grid methods and this justifies the use of unstructured grids in spite of the relative inefficiency of computation.

The focus of the present research is to study the influence of installed nacelle on the flowfield over wing, and only the wing and pylon-mounted nacelle are modeled without the fuselage and tail to save the memory requirement and computer time. In Figure 8, the surface triangular mesh of

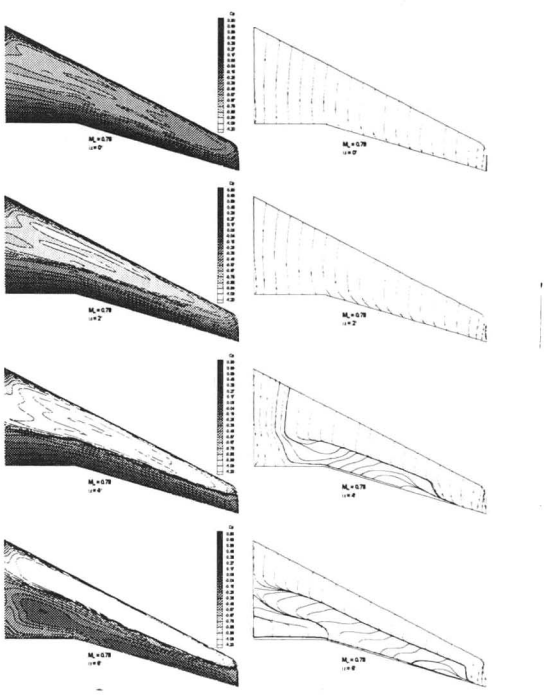

Fig. 7. Contour Plots of Pressure Coefficient and Streamline Patterns on the Upper Surface of the K100-04A at M=0.85, Re=2.45×10^7

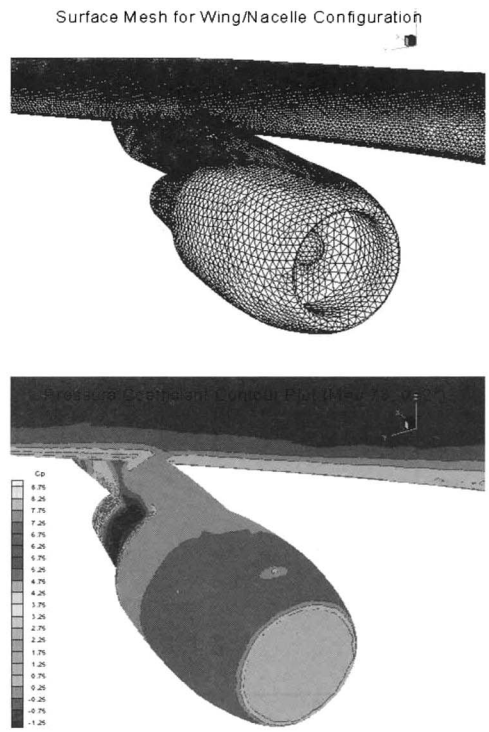

Fig. 8. Triangular Surface Mesh and Pressure Contour Plot of K100-04A Wing with Installed Nacelle

the wing and nacelle is shown with the pressure coefficient contours at Mach number of 0.78 and angle of attack of 2°. The boundary conditions are specified using the data from the engine manufacturer, and total pressure, total temperature and flow angle are specified at nozzle and fan exit while static pressure is specified at fan inlet. The surface triangular mesh shown in Figure 8 consists of 41,472 nodes on the wing and 13,876 nodes on nacelle, and the total number of tetrahedral mesh is about 670,000.

To see the influence of nacelle installation, the flow around the wing without nacelle was first computed for cruise Mach number of 0.78 and angle of attack of 2°. Then, the flow around the wing with nacelle is computed and compared with the previous result. Three streams of flow with different total pressure from freestream, fan exit, and core exit interact at rear core cowl as shown in the contour plot in Figure 8. Very complex flow pattern is observed in this region, but no more explanation is given here as it is not the primary area of interest in this study. The interaction of wing and nacelle can be clearly seen in Figure 9 where the pressure coefficient distributions with and without nacelle at a few spanwise locations are compared. As expected, the strongest influence is observed near the pylon/wing junction region (η=0.3874 is where the wing is cranked and the junction is slightly inboard of this), and the flow pattern on the lower surface is completely altered. The influence of nacelle installation is more significant in inboard region than in outboard region. In inboard region, the pressure distribution on both upper and lower surfaces are significantly changed while the effect of nacelle is more pronounced on the upper surface in outboard region. On the upper surface in both inboard and outboard regions, the influence of nacelle makes shock move upstream and slightly weaker in strength. The lift generated by wing is decreased as expected by approximately 10% due to the influence of nacelle installation for this configuration. It is interesting that the drag coefficient of wing is also decreased. This can be attributed to the reduced shock strength all over the upper wing surface resulting in the decrease in wave drag. But the overall drag coefficient including nacelle increases even without incorporating the viscous effect.

Conclusions

The effort using CFD for accurate prediction of the aerodynamic coefficients of an aircraft in the preliminary design stage together with the prediction of the flowfield under the influence of wall interference was outlined. The accuracy of the three Navier-Stokes codes, employing multi-block, overset, and unstructured grid methods respectively, was first demonstrated by comparison with the experimental data of the transonic flowfield about RAE wing/fuselage configuration.

The multi-block code was used to provide the detailed data on the flowfield around KARI wall interference model with different test section sizes which would be used in establishing the wall interference correction method. The effect of wall interference in the lift and drag coefficients was well predicted. The influence of the presence of test section walls was most pronounced around the leading edge of main wing, and it was almost negligible on the flap and fuselage away from main wing.

The Chimera overset grid solver was applied to provide the aerodynamic coefficients of wing/fuselage/tail configuration of K100-04A for both subsonic and transonic flow conditions. The results for subsonic flows were compared with those of wind tunnel test, and the agreement was found to be excellent. For transonic flows of cruise condition,

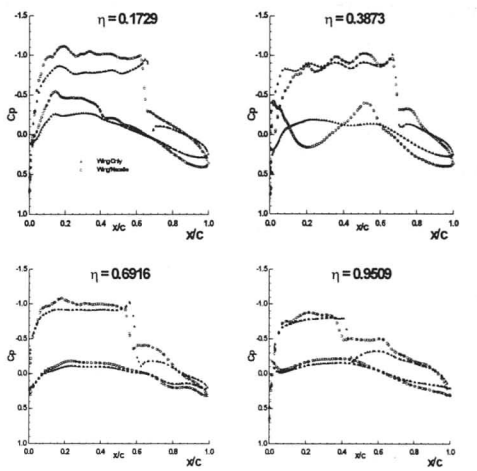

Fig. 9. Comparison of Pressure Coefficient Distributions On the Wing With and Without Nacelle

shock-induced boundary layer separation was predicted which caused decrease in the slope of the lift coefficient curve.

The interference effect of nacelle installation on the wing of K100-04A was also investigated using the unstructured grid method, and about 10% reduction in wing lift was observed. The influence of nacelle was more pronounced in inboard region than in outboard region, and the position of shock moved upstream with weaker strength. The drag coefficient by wing only for the wing/nacelle configuration was also decreased, and this could be attributed to the reduced shock strength. But the overall drag coefficient including nacelle increased even without the viscous effect.

Acknowledgement

This research was supported by the Ministry of Commerce, Industry and Energy of Korea under the grant G96020, and most of the computation was done using the Cray-C90 supercomputer at KORDIC (Korea Research and Development Information Center, Taejon, Korea).

References

1. Venkatakrishnan, V., "Perspective on Unstructured Grid Flow Solvers," *AIAA Journal*, Vol. 34, No. 3, March 1996.

2. Kao, T. J., Su, T. Y., and Yu, N. J., "Navier-Stokes Calculations for Transport Wing-body Configurations with Nacelles and Struts," AIAA Paper 93-2945, 1993.

3. Benek, J. A., Buning, P. G., and Steger, J. L., "A 3-D Chimera Grid Embedding Technique," AIAA Paper 85-1523, 1985.

4. *Engineering Sciences Data Unit*, ESDU International plc, London, England.

5. *The USAF Stability and Control Digital DATCOM*, Volume I, McDonnel Douglas Astronautics Company.

6. Kim, I. "Development of the Aerodynamic Design and Analysis Techniques of a High Speed Train," UCN94220, KARI Technical Report, 1994.

7. Choi, S. and Sung, B, "Analysis of Inviscid Flow Around an Aircraft Using Chimera Grid Technique," *Journal of the Korean Society for Aeronautical and Space Sciences*, Vol. 23, No. 5, 1995.

8. Kwon, O. and Rho, O, "Viscous Flow Calculations With k-e turbulence Closure on Unstructured Triangular Meshes," *Journal of the Korean Society for Aeronautical and Space Sciences*, Vol. 24, No. 4, 1996.

9. Frink, N. T., "Upwind Scheme for Solving the Euler Equations on Unstructured Tetrahedral Meshes," *AIAA Journal*, Vol. 30, No. 1, 1992.

10. Treasgold, D. A., Jones, A. F., and Wilson, K. H., "Pressure Distribution Measured in the RAE 8 ft 6 ft Transonic Wind Tunnel on RAE Wing A in Combination with an Axi-symmetric Body at Mach Numbers of 0.4, 0.8, and 0.9," AGARD-AR-138, May 1979, Chapter B-4.

11. Labrujere, Th. E., Maarsingh, R. A., and Smith, J., "Evaluation of Measured-Boundary-Condition Methods for 3D Subsonic Wall Interference," NLR TR 88072 U, National Aerospace Laboratory NLR, the Netherlands, 1988.

12. The GRIDGENeration Experts^{TM}, Pointwise, Inc., Texas, U.S.A.

13. Sung, B. et al., "K100-04A Screen Test (1)," KARI-TR-AD-97006, Korea Aerospace Research Institute, 1997.

14. Kim, I, Chung, J. D., and Choi, S., "Computational and Experimental Investigation of the Flowfields about High Speed Train Configuration," *Journal of the Korean Society for Aeronautical and Space Sciences*, Vol. 25, No. 6, 1997.

15. Pate, L., Lecordix, J. L., and Dessale, B., "CFD Tools for Designing Isolated and Installed Nacelles," AIAA Paper 95-2625, 1995.